Frequency upconversion of Tm^{3+} and Yb^{3+} codoped $YLiF_4$ synthesized by hydrothermal method

Xiaojiang Pei [a,b,*], Yanbing Hou [a,b], Suling Zhao [a,b], Zheng Xu [a,b], Feng Teng [a,b]

[a] *Institute of Optoelectronic Technology, Beijing Jiaotong University, Beijing 100044, PR China*
[b] *The Lab of Materials for Information Storage and Displays, Beijing 100044, PR China*

Abstract

In this paper, $YLiF_4$ codoped with Tm^{3+} and Yb^{3+} ions was synthesized by hydrothermal method. Yb^{3+} concentration is fixed at 1.5%, and Tm^{3+} concentration is changed from 0.1 to 0.4%. Intense upconversion luminescence is observed when the samples are excited by 980 nm. The dependence of upconversion luminescence on Tm^{3+} concentrations is presented. The results show that upconversion luminescence increases with the Tm^+ concentration and gets its peak at 0.3 mol%. Under the excitation of 980 nm, the blue emission of 479 nm and the red emission of 647 nm are both duo to two photons process, and the UV emission of 361 nm is attributed to the three photons process. We also analyse the upconversion mechanism and process.
© 2004 Elsevier B.V. All rights reserved.

Keywords: Upconversion luminescence; Hydrothermal synthesis; $YLiF_4$:Tm^{3+}, Yb^{3+}

1. Introduction

In recent years, much attention has been devoted to the development of infrared to visible upconversion lasers and fibre amplifiers [1–3]. Many trivalent rare earth ions such as Er^{3+} [4–6], Tm^{3+} [7,8] and Pr^{3+} [9] are doped as emission and absorption centres in these materials. Among the rare earth ions, Yb^{3+} becomes the most suitable sensitizer ions because of its special energy levels and long excited level life.

When a rare earth-doped optical device is developed, the host material is a very important factor to be considered. So far, much effort has been put into fluoride systems owing to their lower phonon energy than oxides [10–12]. In the past, the synthetical methods of fluoride materials include solid-state reaction [11–13] and sol–gel synthesis [14] basically. For fluoride materials, both solid-state reaction and sol–gel synthesis are unsuitable methods [15]. There are two reasons to explain it. One is that the processing of solid-state reaction needs high temperature and protecting atmosphere, which is very critical for electric furnace. If not so, a fluoride material is very easily to be oxidized. The other one is about the sol–gel synthesis. Considering the gel processes

used for preparing oxide materials, it is apparent that it is not possible to have a direct analogy to the oxide route for fluorides, since the analogue of an alkoxide does not exist for monovalent fluorine, and the intermetallic bridging capacity of the fluorine atom is considerably less than that of oxygen.

In our present study, we developed a fluoride $YLiF_4$ codoped with Tm^{3+} and Yb^{3+} ions prepared by hydrothermal synthesis. Hydrothermal synthesis method is a new method for preparation of upconversion host materials. To our best knowledge, works on the upconversion luminescence host material synthesized by hydrothermal have been reported only in our group. In this paper, we also investigated the absorption and upconversion properties of $YLiF_4$:Tm^{3+}, Yb^{3+}. From these spectra, conclusion can be drawn that hydrothermal synthesis for upconversion host materials is a promising synthesizing method.

2. Experiments

The composition of the investigated fluorides were prepared by hydrothermal synthesis as following procedure: $(0.985 - x)Y_2O_3 + 2LiF + 3NH_4HF_2 + xTm_2O_3 + 0.015YbCl_3 = 2Y_{(1-x)}Tm_xLiF_4 + 3NH_3 + 3H_2O$ (mol%). x varies from 0.001 to 0.004 mol. The starting materials

have purity at least 99.9%. Mixed and stirred them together, then, a small mount of hydrofluoric acid was added to adjust the pH value of the initial mixture in order to optimize the reaction conditions. The mixture was sealed in Teflon-lined stainless-steel autoclaves and heated at 220 °C for 96 h. After the reaction, the products ware filtered, washed with distilled water and alcohol, and were dried at room temperature.

The X-ray powder diffraction pattern was recorded on a Dmax X-ray diffractometer using monochromated Cu Kα 1 radiation. The SEM spectrum was also measured with S650 scanning electron microscope. The absorption and upconversion spectra were measured with UV-3101PC spectrophotometer and Spex, respectively. All measurements were carried out at room temperature, and no spectral correction was done.

Fig. 2. SEM spectrum of YLiF$_4$ sample.

3. Result and discussion

Fig. 1 shows the X-ray powder diffraction pattern of YLiF$_4$:Tm^{3+}, Yb^{3+} prepared by hydrothermal method. It is basically consistent with the standard X-ray diffraction card JCPDS 17-874, indicating good synthesis of samples and pimping effects of the rare earth ions to the samples. The SEM spectrum is shown in Fig. 2. It reveals that the crystal lattice has a structure of foursquare scheelite and the grain bulk is well-proportioned.

Fig. 3 illustrates the absorption spectra in the 200–1700 nm wavelength range at room temperature, obtained from YLiF$_4$:Tm^{3+}, Yb^{3+} with different Tm^{3+} concentrations. These absorption peaks centre around 1681, 1210, 786, 685 and 467 nm, corresponding to the following transitions from ground state $^3H_6$ to excited states: $^3H_4$, $^3H_5$, $^3F_4$, $^3F_{2,3}$ and $^1G_4$ of Tm^{3+}. The broad peak about 980 nm can be assigned to $^2F_{7/2} \rightarrow {}^2F_{5/2}$ transition of Yb^{3+}. In addition, there is also a peak around 1403 nm which can be eliminated after
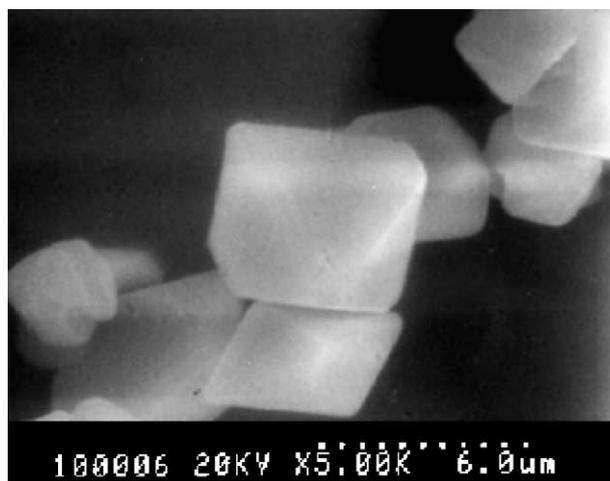
annealing, and we cannot find any suited levels of Tm^{3+}, so we can affirm that the peak is not a absorption peak of Tm^{3+} but a peak of some impurity in the host material. The absorption intensities become stronger along with the increasing of Tm^{3+} concentration. The spectra fluctuation between 830 and 950 nm is derived from the switch around 840 nm of the detectors.

In Fig. 4, room temperature upconversion fluorescence spectra of YLiF$_4$:Tm^{3+}, Yb^{3+} with different concentration of Tm^{3+} in the wavelength region of 300–700 nm are shown, for a pump current of 900 mA coupled into the samples. As can be observed, the upconversion fluorescence exhibit similar spectral contents as far as emission wavelength are concerned, and the signal light emanating from the sample presented four distinct emission bands centred around 361, 450, 479 and 647 nm, corresponding to the $^1D_2 \rightarrow {}^3H_6$, $^1D_2 \rightarrow {}^3H_4$, $^1G_4 \rightarrow {}^3H_6$ and $^1G_4 \rightarrow {}^3H_4$ transitions of Tm^{3+}, respectively, as illustrated in the simplified energy-level diagram for the Tm^{3+}/Yb^{3+} pair of Fig. 5. It is important to
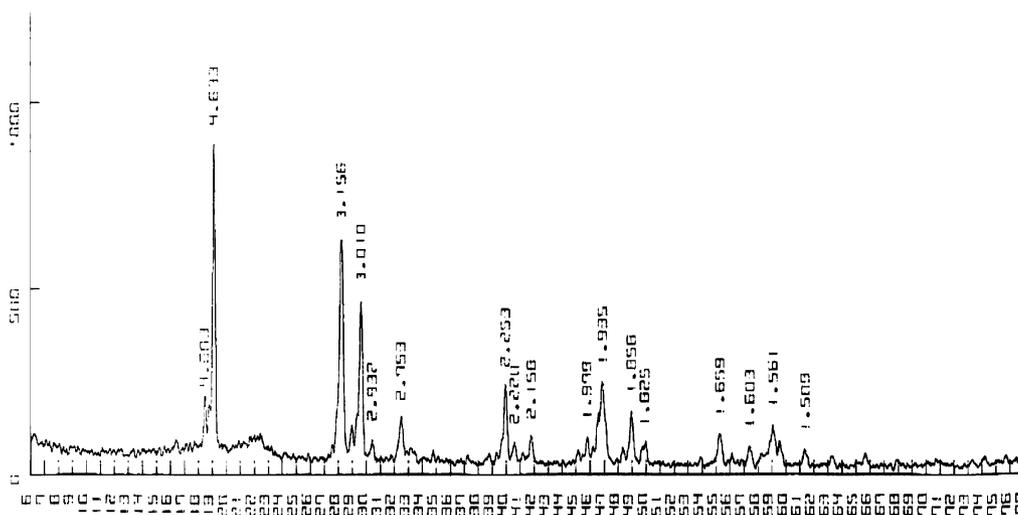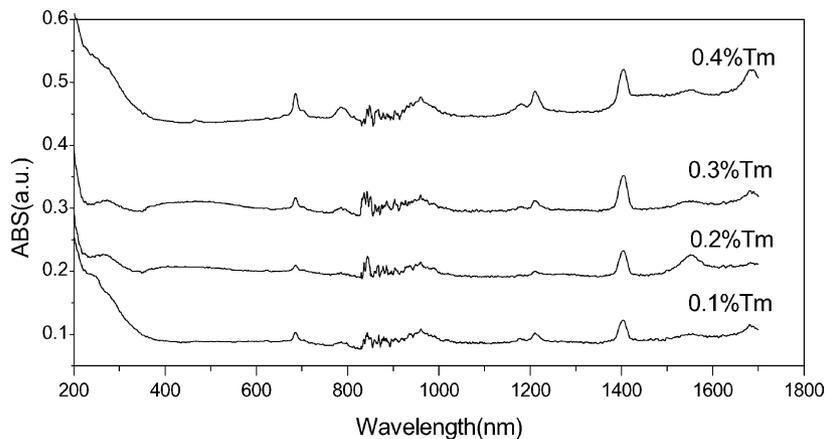

Fig. 1. XRD spectrum of YLiF$_4$ sample.

Fig. 3. Room temperature absorption spectra of YLiF$_4$:Tm, Yb samples with different Tm^{3+} concentration.
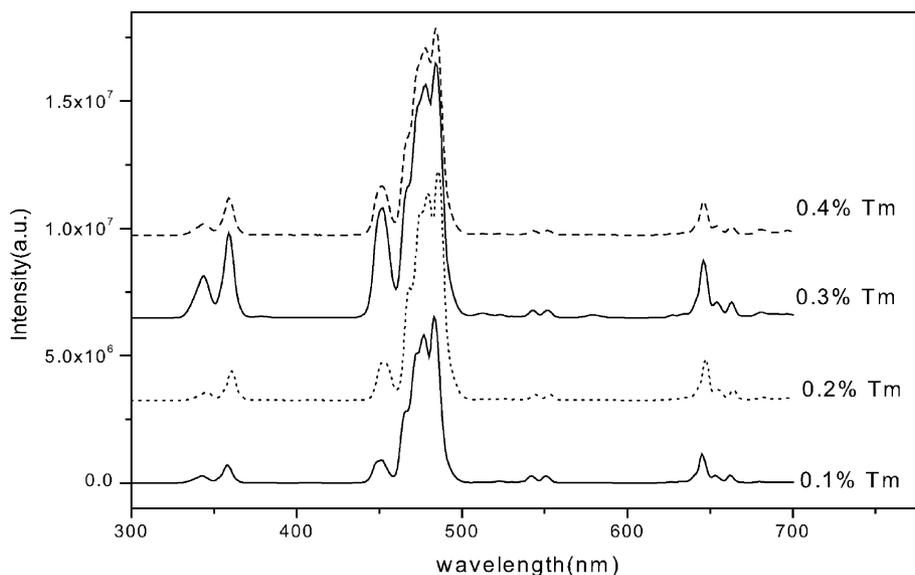

Fig. 4. Room temperature frequency upconversion spectra of YLiF$_4$:Tm, Yb excited by 980 nm.

mention at this point that the blue emission around 479 nm is intense enough to be seen by naked eyes, for pump power of a few tens of milliwatts with day-light illumination in the laboratory. We also observed that the emission intensity reach its peak with Tm^{3+} concentration of 0.3 mol%, and concentration quenching occurs above this concentration. This is maybe duo to the cross-relaxation between Tm^{3+} ions and the existing of OH^{-} because of water in our experiment.

For any process of upconversion luminescence, the visible output intensity I_{VIS} is approximately proportional to the power n of infrared excitation intensity I_{IR}, i.e., $I_{VIS} \propto I_{IR}^{n}$. In a double-log coordinate, the slope of I_{VIS}–I_{IR} indicates n that reveals the responsive relation between IR excitation light and visible (VIS) emission. Fig. 6 shows the dependencies of the upconversion intensities upon pump power for the samples with different Tm^{3+} concentration According to the value of n obtained from the power law, both the red (647 nm) and blue (479 nm) radiation originate from processes involving two photons ($n \sim 2$) and the UV (361 nm)

radiation originates from process involving three photons ($n \sim 3$). The difference of slope between different Tm^{3+} concentration maybe is ascribed to the error of measurement condition and fit linear. From many literatures before such as [16], the blue emission of 479 nm is deemed to originate from process involving three photons with mechanism of phonon-assistant energy transfer. In our research, its interesting that the 479 nm emission is a process involving two phonons. We consider the mechanism a cooperative sensitization process because the energy of $^1G_4$ level is almost equal to the sum of two 980 nm photons, considering the broadening of energy levels. This mechanism will be discussed in detail later.

The upconversion mechanisms involved in the population of the relevant excited state emitting levels of the Yb/Tm codoped materials are described in Fig. 8. Two 980 nm photons are absorbed by two Yb^{3+}, respectively, exciting Yb^{3+} ground state $^4F_{5/2}$ to excited state $^4F_{7/2}$, then transfer their energies to one nearby Tm^{3+}, exciting it to the excited state
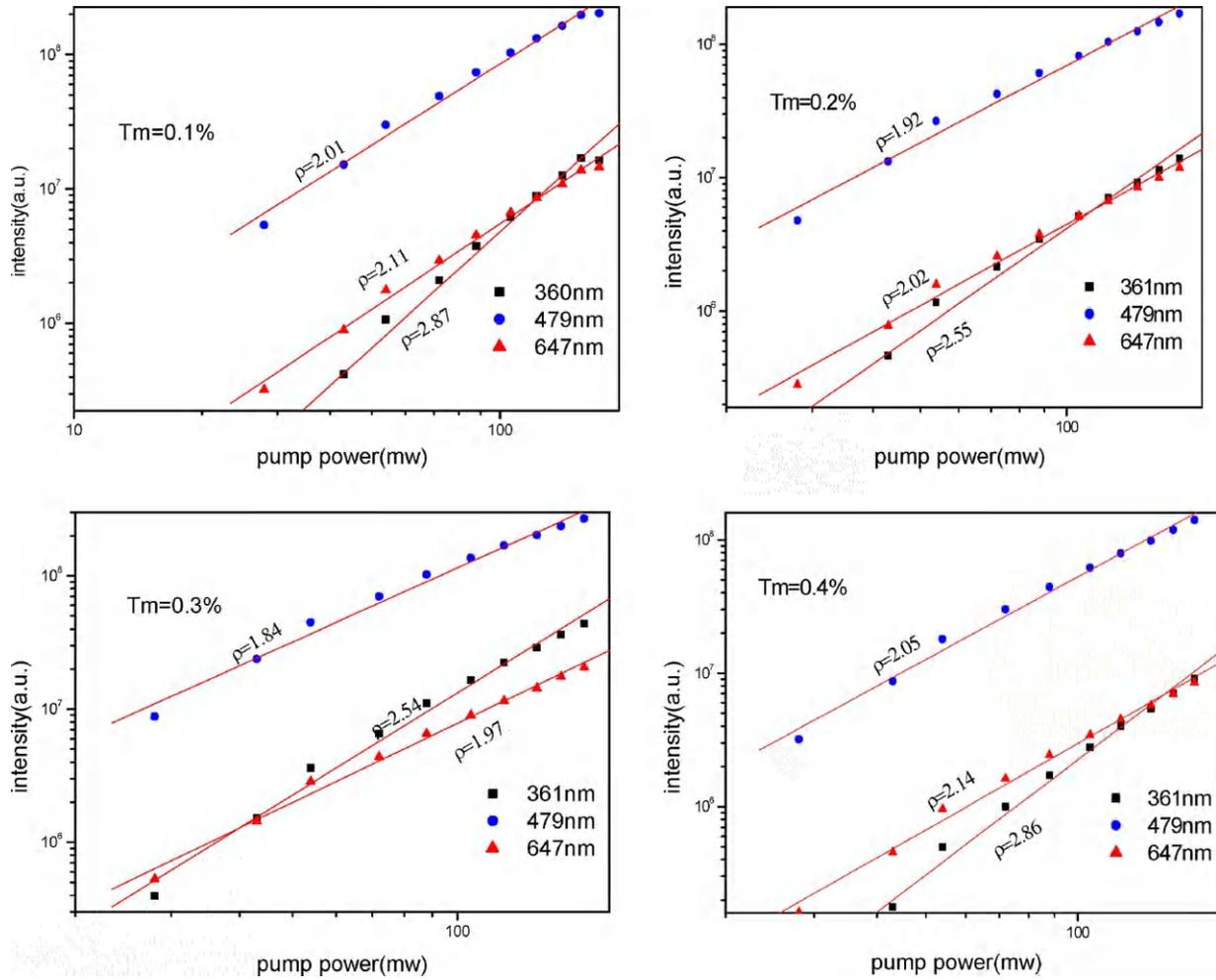
Fig. 5. Energy-level scheme for the Tm/Yb-pair indicating the possible mechanism of cooperative sensitization and phonon-assistant energy transfer. The bold arrows represent the emission, and the dashed arrows represent cooperative sensitization.
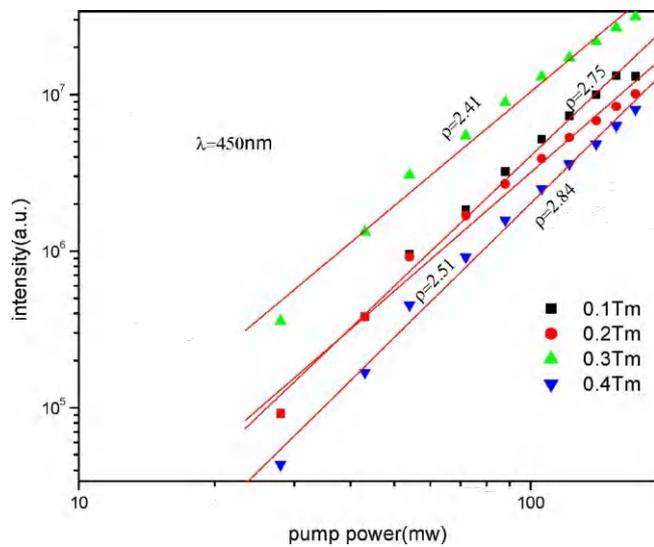

Fig. 6. Log–log plot of frequency upconversion emission intensity as a function of the excitation power at 980 nm for the YLiF4:Tm, Yb samples at room temperature.
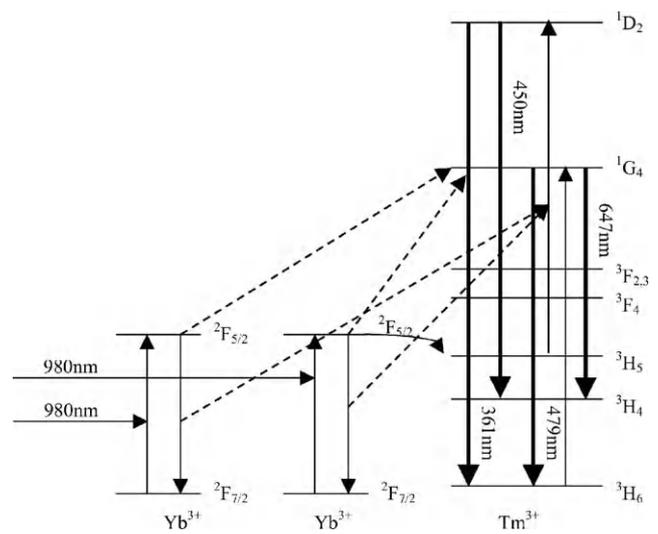

Fig. 7. Log–log plot of 450 nm emission intensity as a function of the excitation power at 980 nm for the YLiF4:Tm, Yb samples at room temperature.

$^1G_4$ corresponding to 479 and 647 nm emission by cooperative sensitization process. The 450 and 361 nm emission can be described as follows: one 980 nm photon is absorbed by one Yb^{3+}, then transfer the energy to one nearby Tm^{3+}, exciting its ground state $^3H_6$ to $^3H_5$ through phonon-assistant energy transfer, then Tm^{3+} reaches the excited state of $^1D_2$ by cooperative sensitization. Fig. 7 shows the double-log curves of 450 nm emission, as can be seen, the slopes are similar to the slopes of 361 nm emission, indicating the 450 nm emission comes from the same level with 361 nm emission of the $^1D_2$ level.

4. Conclusions

In conclusion, the upconversion of the 980 nm wavelength to visible one was studied for $YLiF_4$ codoped with Tm^{3+} and Yb^{3+} ions synthesized by hydrothermal method. The upconversion luminescence increases with the Tm^+ concentration and gets its peak at 0.3 mol%, then decreases with the increasing of Tm^+ concentration. Under the excitation of 980 nm, the blue emission of 479 nm and the red emission of 647 nm are both due to two photons process by cooperative sensitization process, and the UV emission of 361 nm is attributed to the three photons process.

References

[1] M.J.L. Digonnet, Rare Earth Doped Fiber Lasers and Amplifiers, Stanford University, Stanford, California, 1993.
[2] E. Snokes, G.N. van den Hoven, A. Polman, IEEE J. Quant. Electron. 32 (1996) 1680.
[3] M. Tsuda, K. Soga, H. Inoue, S. Inoue, A. Makishima, J. Appl. Phys. 85 (1999) 29.
[4] H. Lin, E.Y.B. Pun, X.R. Liu, J. Non-Cryst. Solids 283 (2001) 27–33.
[5] C.T.M. Ribeiro, A.R. Zanatta, L.A.O. Nunes, et al., Optical spectroscopy of Er^{3+} and Yb^{3+} co-doped fluoroindate glasses, J. Appl. Phys. 83 (4) (1998) 2256–2260.
[6] A.S. Oliveira, M.T. de Araujo, A.S. Gouveia-Neto, et al., Frequency upconversion in Er^{3+}/Yb^{3+}-codoped chalcogenide glass, Appl. Phys. Lett. 72 (7) (1998) 753–755.
[7] S. Huang, S.T. Lai, L. Lou, et al., Upconversion in $LaF3:Tm^{3+}$, Phys. Rev. B 24 (1) (1981) 59–63.
[8] J.J. Owen, A.K. Cheetham, R.A. McFarlane, Orientation-dependent fluorescence studies and spectroscopic analysis of doped barium yttrium fluoride upconversion laser crystals $BaY_{2-x-y}Yb_xTm_yF_8$, J. Opt. Soc. Am. B 15 (2) (1998) 684–693.
[9] E. Pecoraro, D.F. de Sousa, R. Lebullenger, et al., Evaluation of the energy transfer rate for the $Yb^{3+}:Pr^{3+}$ system in lead fluoroindogallate glasses, J. Appl. Phys. 86 (6) (1999) 3144–3148.
[10] N. Rakov, C.B. de Araujo, Y. Messaddeq, M.A. Aegerter, Avalanche upconversion in Er^{3+}-doped fluoroindate glass, Appl. Phys. Lett. 70 (23) (1997) 3084–3086.
[11] C.T.M. Ribeiro, A.R. Zanatta, L.A.O. Nunes, et al., Optical spectroscopy of Er^{3+} and Yb^{3+} co-doped fluoroindate glasses, J. Appl. Phys. 83 (4) (1998) 2256–2260.
[12] D.F. de Sousa, L.F.C. Zonetti, M.J.V. Bell, et al., $Er^{3+}:Yb^{3+}$ codoped lead fluoroindogallate glasses for mid infrared and upconversion applications, J. Appl. Phys. 85 (5) (1999) 2502–2507.
[13] B.C. Collings, A.J. Silversmith, Avalanche upconversion in $LaF3:Tm^{3+}$, J. Lumin. 62 (1994) 271–279.
[14] P.J. Melling, M.A. Thomson, Sol–gel preparation of amorphous ZBLA heavy metal fluoride powders, J. Mater. Res. 5 (5) (1990) 1092–1094.
[15] X. Ruren, P. Wenqing, Wuji Hecheng yu Zhibei Huaxue, Higher Education Press, 2001 (in Chinese).
[16] F. Auzel, Computeur quantique part transfer d'energie de Yb^{3+} and Tm^{3+} dans un tungstate mixte et dans un verre germanate, C.R. Acad. Sci. 4 (1966) 317–318.